

Magma Intrusion Beneath Long Valley Caldera Confirmed by Temporal Changes in Gravity

M. Battaglia,^{1*} C. Roberts,² P. Segall¹

Precise relative gravity measurements conducted in Long Valley (California) in 1982 and 1998 reveal a decrease in gravity of as much as -107 ± 6 microgals (1 microgal = 10^{-8} meters per square second) centered on the uplifting resurgent dome. A positive residual gravity change of up to 64 ± 15 microgals was found after correcting for the effects of uplift and water table fluctuations. Assuming a point source of intrusion, the density of the intruding material is 2.7×10^3 to 4.1×10^3 kilograms per cubic meter at 95 percent confidence. The gravity results require intrusion of silicate magma and exclude in situ thermal expansion or pressurization of the hydrothermal system as the cause of uplift and seismicity.

Calderas are collapse structures associated with the world's largest volcanic eruptions (1). Several Quaternary calderas exhibit signs of restlessness, including seismicity and uplift, which may last for tens of years (Fig. 1). Uplift at better studied shield volcanoes is unambiguously associated with magma accumulation in the shallow crust (2). The fact that some calderas have subsided without eruption or clear evidence of intrusion into the adjacent crust [Campi Flegrei (3) and Yellowstone (4); see Fig. 1] has led some to suggest that the uplift and seismicity are caused by perturbations to the calderas' hydrothermal systems rather than intrusion of magma (5, 6).

Differentiating between magmatic intrusion on the one hand and thermal expansion or pressurization of the caldera hydrothermal system on the other is critical for accurate assessment of volcanic hazards. Only repeated microgravity measurements can discriminate between these processes (7). Before gravity changes can be interpreted, however, they must be corrected for the effects of uplift (the free-air correction) and changes to the depth of the water table (7, 8). The resultant, or residual, gravity changes can be used to constrain the density and mass of the deformation source (9). Direct measurements of water table changes are rare (8), leading to various strategies to minimize this effect (10).

Long Valley caldera (Fig. 2), located on the eastern front of the Sierra Nevada range in California, formed by collapse of the roof of the magma chamber during the catastrophic eruption of the Bishop Tuff 0.73 million years ago (Ma) (11). Since mid-1980, the caldera has experienced ground uplift (Fig. 1)

and numerous earthquake swarms, prompting the U.S. Geological Survey (USGS) to issue a "Notice of Potential Volcanic Hazard" for a few months in 1982 and to start an intensive monitoring effort in the area (12). Modeling of the ground deformation (13) and seismicity (14) suggests inflation of a magma reservoir beneath the caldera.

The precise gravity network in Long Valley (15), which extends from the Sierra Nevada west of Lee Vining to the White Mountains east of Bishop (Fig. 2), was surveyed annually from 1980 to 1985 (8). Earlier efforts at detecting and interpreting gravity changes were hampered by the small accumulated signal and the difficulty in correcting for shallow groundwater fluctuations, which may overwhelm gravity changes due to intrusion (8). During the July 1998 survey, we measured 34 gravity stations (Fig. 2). Each station was measured with two LaCoste-Romberg gravimeters during two complete loops per day, with the reference station measured three times per day. Data reduction included the removal of solid Earth tides and daily gravimeter drift (16). Between July 1982 and July 1998, gravity within the caldera decreased substantially (Fig. 3A),

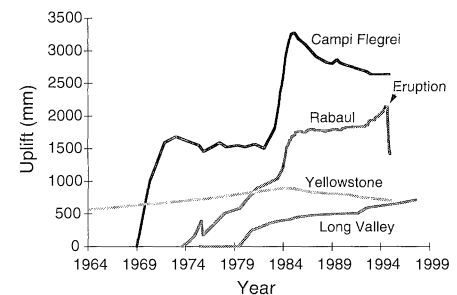
whereas three control stations located on stable granite outcrops more than 5 km outside the caldera showed no substantial change (Table 1). The stations with the largest gravity decrease are all located on the resurgent dome, which has experienced uplift during the past 20 years (Fig. 3B).

Long-term monitoring programs for ground deformation (13) and groundwater level (17) were established by the USGS between 1980 and 1982 (Fig. 2). Water level is measured in shallow wells three times a year (usually in May, July, and November). Complete or partial leveling of Long Valley caldera occurred in 1975, each year from 1980 to 1992, 1995, and 1997 (18). We estimated the uplift between July 1997 and July 1998 using the elastic deformation model of Langbein *et al.* (13), based on two-wavelength geodimeter data. Despite the extensive monitoring effort, water level and uplift data are sparse or nonexistent at most gravity stations over the July 1982 to July 1998 period of interest. For example, only eight gravity stations along Highway 395 and Highway 203 were leveled in 1982 and 1997.

We used kriging (19), an interpolation method, to estimate the uplift at each of the gravity sites for which direct measurements are lacking. The accuracy of the kriging interpolation can be tested by cross validation (Fig. 4A). With cross validation, a level benchmark is omitted from the estimation. The kriging estimate at that point is then compared with the true value. Along Highway 395, the root mean square cross-validation errors were about 20 mm. We estimated the uncertainty in the free-air corrections by modeling the probability distribution of the uplift, conditional on the existing data, through sequential Gaussian simulation (19, 20). The stated uncertainties in the free-air corrections are based on the standard deviation of the simulated uplift. In general, the kriging estimates are accurate at gravity sites close to leveling benchmarks but are poor at sites distant from the leveling lines (Fig. 3B).

The water table contribution to the measured gravity changes is estimated with

Fig. 1. Unrest at large Quaternary silicic calderas. Campi Flegrei, Italy: elevation changes near Pozzuoli (central caldera floor). The ground subsided 0.22 m between mid-1972 and the end of 1974 and 0.5 m after the rapid uplift in 1982–84 (33). Long Valley: The figure shows uplift at the resurgent dome (benchmark 12DOR75) with respect to a point outside the caldera (Lee Vining) (78). Rabaul, Papua New Guinea: elevation changes at the southern tip of Matupit Island (central caldera floor) [(30) and *Bulletin of Global Volcanism Network* from 1983 to 1994]. Yellowstone (Wyoming): elevation changes at Sour Creek dome. The central part of the Yellowstone caldera rose at least 0.7 m during the interval between 1923 and 1976. Uplift stopped in 1984–85, turning to subsidence in 1985–86. Subsidence has exceeded 0.2 m over the entire caldera (4). Between August 1995 and September 1996, the northeast section of the caldera began to reflate (6).



¹Department of Geophysics, Stanford University, Stanford, CA 94305, USA. ²U.S. Geological Survey, Menlo Park, CA 94025, USA.

*To whom correspondence should be addressed.

REPORTS

space-time kriging (21) to interpolate the depth to the water table at each of the gravity sites at the times of the gravity surveys. Cross validation indicates that, at least in some cases, kriging provides a good estimate of the water level history (Fig. 4, B and C, and Table 2). Porosity is assigned to each site on the basis of the local rock type: 5% for granite outcrops, 10% for volcanic flows, and 45% for unconsolidated sediments (22). The net effect on the gravity measurements is small, typically 1 to 4 μgal , the largest being

-7 μgal . The uncertainties in the water table correction depend on how close the site is to a monitoring well, the quality of the data from that well, and the porosity. Estimated errors, based on simulation of the water table level histories and assuming a 10% uncertainty in the porosity, range from a low of 3 μgal on granite and rhyolite outcrops to a maximum of 57 μgal for one sediment site.

The residual gravity field shows a prominent positive anomaly centered on the resurgent dome (Fig. 3C) with a peak amplitude of

$64 \pm 16 \mu\text{gal}$. The anomaly is defined by gravity changes in excess of 40 μgal at five stations (Fig. 3C). The variance of the residual gravity change is the sum of the measurement variance, the variance of the free-air correction, and the variance of the water table correction. The secondary maximum of $58 \pm 44 \mu\text{gal}$ in the eastern caldera is due primarily to a single station. The large uncertainty in the free-air correction and water table change at this site, as well as possible systematic errors, suggests that the secondary maximum

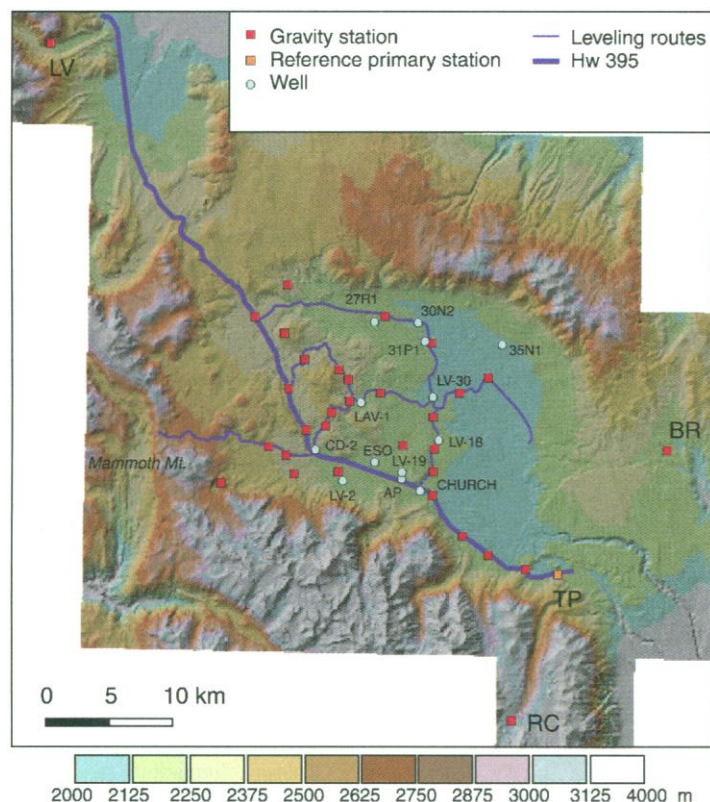
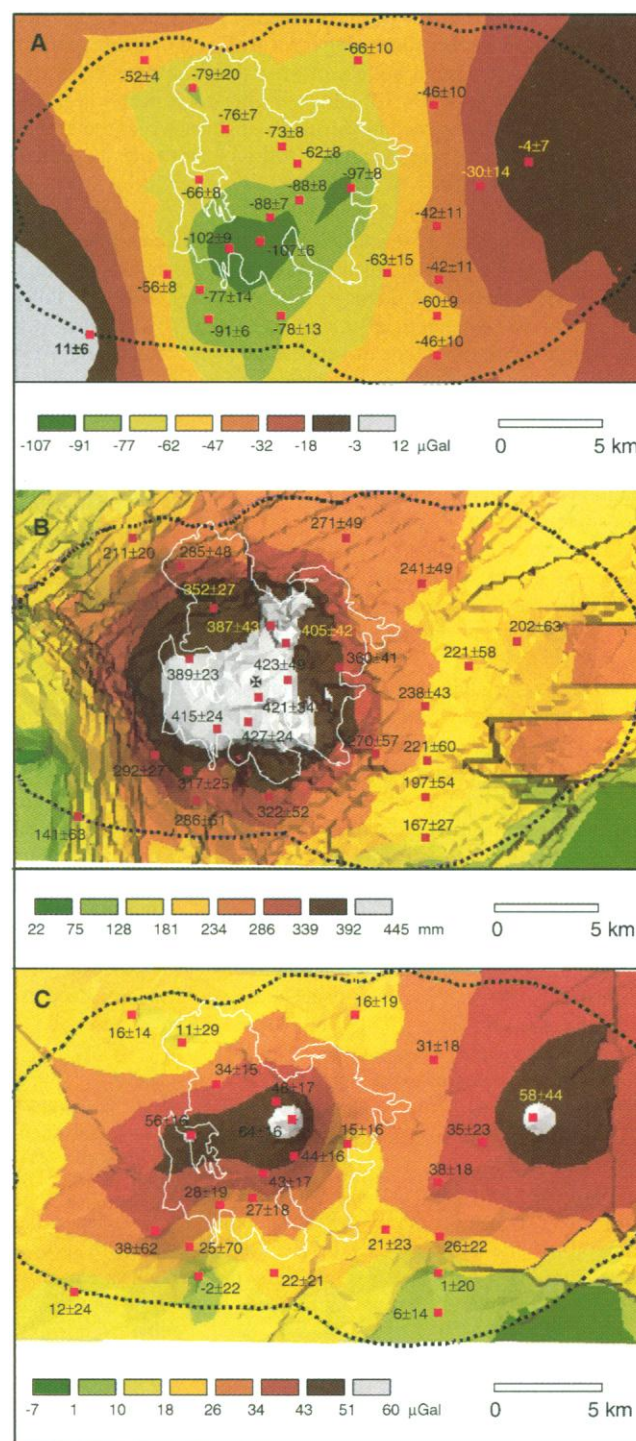


Fig. 2 (above). Map of Long Valley caldera showing networks for monitoring gravity, uplift, and groundwater level. Gravity stations: BR, Benton Range; LV, Lee Vining; RC, Rock Creek Lake; and TP, Tom's Place. All gravity readings were taken relative to Tom's Place. About 0.1 million years after the caldera collapse, renewal of magma pressure at depth uplifted the central part of the caldera floor, forming a resurgent dome about 10 km in diameter and 500 m high (11). Mammoth Mountain, a quiescent dacitic volcano, is the site of a diffuse CO_2 emission, responsible for killed trees over a 30-ha area (34). **Fig. 3 (right).** (A) Gravity changes (in microgals) in Long Valley caldera from July 1982 to July 1998. Measured values and 1 SD errors are indicated. The white line marks the resurgent dome boundary. (B) Uplift at Long Valley caldera between 1982 and 1998. The small area of relative subsidence in the south moat is due to fluid withdrawal from the Casa Diablo geothermal field (35). Estimated uplift and 1 SD errors are indicated at the gravity stations. The cross marks the location of the model point source. The white line marks the resurgent dome boundary. (C) Residual gravity changes in Long Valley caldera from July 1982 to July 1998. Estimated values and 1 SD errors are indicated. The white line marks the resurgent dome boundary.



REPORTS

should be viewed with caution (23).

The positive residual gravity (Δg_R) signal suggests intrusion into the subcaldera crust. We estimated the depth of the intrusion assuming a simple spherically symmetric point source (9) (Fig. 5A), although we do not preclude more complex models:

$$\Delta g_R = G\Delta M \frac{d}{(d^2 + r^2)^{3/2}} \quad (1)$$

Here G is the gravitational constant, ΔM is the mass of the intrusion, d is the depth of the intrusion, and r is the horizontal distance from the point source. This gives a depth of 10.6 km and a mass of 7.4×10^{11} kg. We used a bootstrap percentile method (24), which yielded 95% confidence bounds on the depth and intrusion mass of 6.9 to 18.3 km and 3.8×10^{11} to 17.8×10^{11} kg, respectively. The estimated source depth agrees with estimates from point source models (25) of the uplift (Fig. 5B). We used only observed height differences from 1982 to 1997, not kriging estimates, in this calculation. This yielded a source depth of 11.6 km (95% bounds of 10.0 to 13.8 km) and a volume increase of 0.22 km^3 (95% bounds of 0.16 to 0.32 km^3).

Given that the uplift and gravity changes are consistent with a single point source, we can estimate the density ρ of the intrusion by (9):

$$\rho = \frac{1 - \nu}{\pi G} \left(\frac{\Delta g}{u_z} - \gamma \right) \quad (2)$$

Table 1. Values at control stations for relative gravity change (change) and residual gravity (residual). All values are given in microgals, and errors are 1 SD.

	Change	Residual
BR	-3 ± 9	25 ± 26
LV	-2 ± 11	-2 ± 17
RC	-5 ± 10	-5 ± 16

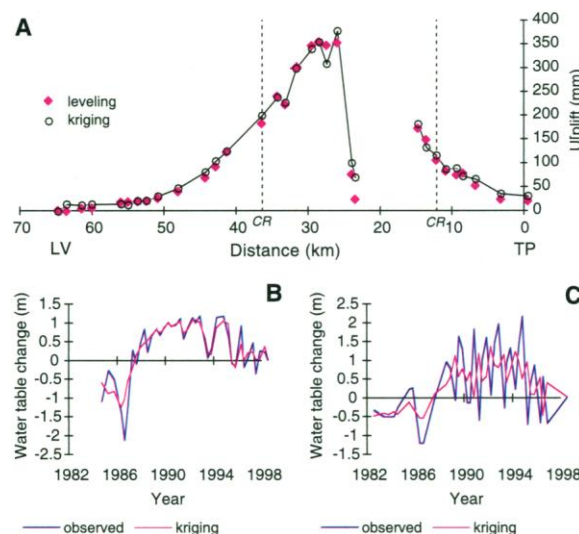
where $\nu = 0.25$ is Poisson's ratio, $\Delta g/u_z$ is the slope of the best fit line for gravity (corrected for water table effects) versus uplift u_z , and $\gamma = 308.6 \text{ } \mu\text{gal/m}$ is the free-air gradient (Fig. 5C). This leads to an estimated density of $3.3 \times 10^3 \text{ kg/m}^3$. The 95% bootstrap confidence bounds on the density are 2.7×10^3 to $4.0 \times 10^3 \text{ kg/m}^3$. The lower end of this range would suggest basaltic intrusion (26); however, the density estimates are conditioned on the point source approximation and thus must be used with some caution. The data do, however, exclude thermo-elastic deformation, which would yield a negligible residual gravity signal (27), or hydrothermal fluids, which would lead to densities much less than estimated.

The volume of the intrusion can be computed by dividing the estimated mass addition (7.4×10^{11} kg) by the estimated density ($3.3 \times 10^3 \text{ kg/m}^3$), which yields 0.22 km^3 (0.11 km^3 to 0.54 km^3 at 95% confidence). This result agrees with the volume change of 0.22 km^3 (95% bounds of 0.16 to 0.32 km^3) estimated from the uplift data (28).

Table 2. Correlation (R) between measurements and cross-validation estimate of changes to the depth of the water table (see Fig. 2 for well location).

Well	R
LV-19	0.93
AP	0.92
CD-2	0.83
LV-18	0.77
27R1	0.74
CHURCH	0.65
31P1	0.64
ESO	0.60
LV-2	0.41
LAV-1	0.31
30N2	0.24
LV-30	-0.48
35N1	-0.54

Fig. 4. (A) Cross-validation estimates of the uplift along Highway 395 compared with the actual leveling data from 1982 to 1997. CR, Caldera Rim; LV, Lee Vining; TP, Tom's Place. (B and C) Examples of cross-validation estimates of changes in the depth of the water table relative to July 1998. Position of wells AP (B) and LAV-1 (C) is shown in Fig. 2. Correlation between experimental data and kriging estimate is 92% for AP and 31% for LAV-1.



The results of the gravity study are consistent with other geophysical and geological observations in Long Valley. Eruption of moat rhyolites at 0.5, 0.3, and 0.1 Ma suggests that the magma chamber is sustained by periodic injection of basalt from the mantle (11). Teleseismic tomography shows a 25 to 30% low-velocity zone centered at 11.5-km depth beneath the resurgent dome and a deeper, more diffuse 15% low-velocity zone at 24.5-km depth (29). The shallow zone has been interpreted to be the residual Long Valley magma chamber, whereas the deeper feature may represent basaltic magmas ponded in the midcrust (29).

The gravity gradients $\Delta g/u_z$ observed in this study of $215 \pm 11 \text{ } \mu\text{gal/m}$ are similar to those measured during inflation episodes at Campi Flegrei, $213 \pm 6 \text{ } \mu\text{gal/m}$ (3), and Rabaul caldera, Papua New Guinea, $216 \pm 4 \text{ } \mu\text{gal/m}$ (30). At Rabaul caldera, samples from the 1997 eruptions showed evidence of mixing of dacite and basalt, the basalt presumed to be freshly intruded (31). In Long Valley, the evidence therefore suggests that basaltic magma has been intrud-

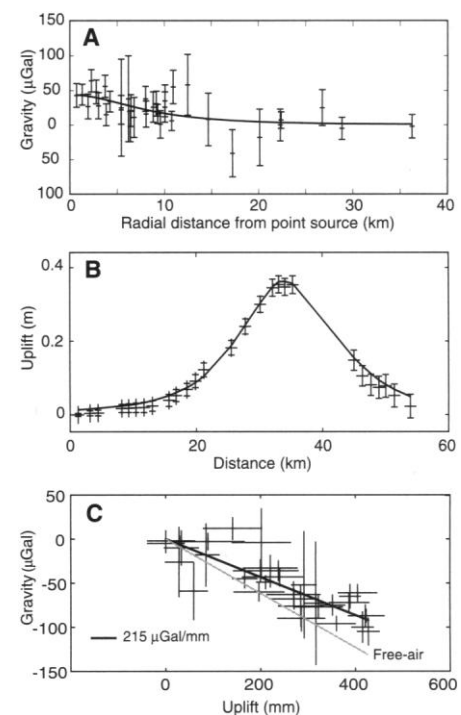


Fig. 5. (A) Comparison of observed and predicted residual gravity change (1982–98), as a function of radial distance from the point source, for a depth of 10.6 km and mass addition of 7.4×10^{11} kg. (B) Comparison of observed and predicted uplift (1982–97) along Highway 395 for a point source at depth of 11.6 km and volume increase of 0.22 km^3 . (C) Best fit line for the point source model used to determine the density of the intrusion. Errors in the uplift and gravity changes were included in the regression. The slope of the best fit line is $-215 \text{ } \mu\text{gal/m}$.

ing the remnants of a rhyolitic magma body beneath the resurgent dome since the beginning of unrest in 1980.

References and Notes

1. R. L. Smith and R. A. Bailey, *Mem. Geol. Soc. Am.* **116**, 613 (1968).
2. R. I. Tilling and J. Dvorak, *Nature* **363**, 125 (1993).
3. G. Berrino, *J. Volcanol. Geotherm. Res.* **61**, 293 (1994).
4. D. Dzurisin, K. M. Yamashita, J. W. Kleinman, *Bull. Volcanol.* **56**, 261 (1994).
5. G. De Natale, F. Pingue, P. Allard, A. Zollo, *J. Volcanol. Geotherm. Res.* **48**, 199 (1991).
6. C. Wicks Jr., W. Thatcher, D. Dzurisin, *Science* **282**, 458 (1998).
7. G. Berrino, H. Rymer, G. C. Brown, G. Corrado, *J. Volcanol. Geotherm. Res.* **53**, 11 (1992).
8. R. C. Jachens and C. W. Roberts, *J. Geophys. Res.* **90**, 11210 (1985).
9. A. A. Eggers, *J. Volcanol. Geotherm. Res.* **33**, 201 (1987).
10. Measurements made in the same month may minimize seasonal variations in water table [F. Arnet *et al.*, *Geophys. Res. Lett.* **24**, 2741 (1997)]; sites on low-porosity outcrops (32) or near sea level (30) may minimize water table effects on gravity changes.
11. R. A. Bailey, *Map I-1933* (U.S. Geological Survey, Reston, VA, 1989).
12. _____ and D. P. Hill, *Geosci. Can.* **17**, 175 (1990).
13. J. Langbein *et al.*, *J. Geophys. Res.* **100**, 12487 (1995).
14. B. R. Julian, *Nature* **303**, 323 (1983).
15. C. W. Roberts, R. C. Jachens, R. Morin, *U.S. Geol. Surv. Rep.* **88-50** (1988).
16. The measured gravity differences at each station were processed with a least squares method to obtain one gravity value following the methods described by R. C. Jachens [in *1980 Eruptions of Mount St. Helens, Washington* (U.S. Geological Survey, Reston, VA, 1981), pp. 175-181].
17. J. F. Howle and C. D. Farrar, *U.S. Geol. Surv. Open File Rep.* **96-382** (1996).
18. D. Dzurisin, personal communication.
19. P. Goovaerts, *Geostatistics for Natural Resources Evaluation* (Oxford Univ. Press, New York, 1997).
20. Kriging provides only an incomplete measure of local accuracy and no estimation of joint accuracy when several locations are considered together. Gaussian simulations are designed specifically to provide such measures. Gaussian simulation is the process of drawing alternative, equally probable, joint realizations of a random variable (in our case, the uplift or change in water table depth at a given location) that follows a multivariate Gaussian distribution. The parameters of the Gaussian distribution (mean and variance) are determined by kriging. The random sampling is such that all the realizations fit the existing data exactly. The variance of a set of simulated values provides a measure of local uncertainty for the attribute of interest.
21. S. Rouhani and D. E. Meyers, *Math. Geol.* **22**, 611 (1990).
22. M. L. Sorey, R. E. Lewis, F. H. Olmsted, *U.S. Geol. Surv. Prof. Pap.* **1044-A** (1978).
23. The fact that the station in the eastern caldera with the large residual gravity change experienced an unusually small raw gravity change ($-4 \pm 7 \mu\text{gal}$) compared with neighboring stations in the eastern caldera (with gravity changes of -46 ± 10 , -30 ± 14 , $-42 \pm 11 \mu\text{gal}$) suggests possible measurement errors at this site (see Fig. 3A).
24. B. Efron and R. Tibshirani, *Stat. Sci.* **1**, 54 (1986). The data were randomly resampled with replacement (that is, some stations appear multiple times and others not at all). The resampled data set was inverted for source depth, and the process was repeated several thousand times. Ninety-five percent confidence intervals were determined by ordering the bootstrap results and excluding the smallest and largest 2.5% of the distribution.
25. K. Mogi, *Bull. Earthquake Res. Inst.* **36**, 99 (1958).

26. R. S. Charnicael, Ed., *Handbook of Physical Rock Properties*, vol. III (CRC Press, Boca Raton, FL, 1984).
27. J. B. Walsh and J. R. Rice, *J. Geophys. Res.* **84**, 165 (1979).
28. The estimated volume from gravity is based on data from July 1982 to July 1998. Because leveling was not conducted in 1998, the estimated volume from leveling is based on data from July 1982 to July 1997. Volume change between 1997 and 1998 is thus not accounted for.
29. C. M. Weiland, L. K. Steck, P. B. Dawson, V. A. Korneev, *J. Geophys. Res.* **100**, 20379 (1995).
30. C. McKee, J. Mori, B. Talai, in *Volcanic Hazards: Assessment and Monitoring* (Springer-Verlag, Berlin, 1989), pp. 399-428.
31. B. Talai *et al.*, *Bull. Global Volcanism Network* **22** (no.

- 4) (1997) (available at http://www.volcano.si.edu/gvp/volcano/region05/newbrit/rabaul/var_01.htm 2204).
32. J. B. Rundle and J. H. Whitcomb, *J. Geophys. Res.* **91**, 12675 (1986).
33. F. Barberi, in *Monitoring and Mitigation of Volcano Hazards* (Springer-Verlag, Berlin, 1996), pp. 771-786.
34. C. D. Farrar *et al.*, *Nature* **376**, 675 (1995).
35. M. L. Sorey, C. D. Farrar, G. A. Marshall, J. F. Howle, *J. Geophys. Res.* **100**, 12475 (1995).
36. This work would have not been possible without support and data from several individuals and institutions. In particular, we thank R. Bailey, D. Dzurisin, C. Farrar, D. Hill, J. Langbein, J. Murray, and W. Thatcher.

28 May 1999; accepted 17 August 1999

Impaired Fas Response and Autoimmunity in *Pten*^{+/-} Mice

Antonio Di Cristofano,¹ Paraskevi Kotsi,¹ Yu Feng Peng,³ Carlos Cordon-Cardo,² Keith B. Elkon,³ Pier Paolo Pandolfi^{1*}

Inactivating mutations in the *PTEN* tumor suppressor gene, encoding a phosphatase, occur in three related human autosomal dominant disorders characterized by tumor susceptibility. Here it is shown that *Pten* heterozygous (*Pten*^{+/-}) mutants develop a lethal polyclonal autoimmune disorder with features reminiscent of those observed in Fas-deficient mutants. Fas-mediated apoptosis was impaired in *Pten*^{+/-} mice, and T lymphocytes from these mice show reduced activation-induced cell death and increased proliferation upon activation. Phosphatidylinositol (PI) 3-kinase inhibitors restored Fas responsiveness in *Pten*^{+/-} cells. These results indicate that *Pten* is an essential mediator of the Fas response and a repressor of autoimmunity and thus implicate the PI 3-kinase/Akt pathway in Fas-mediated apoptosis.

The *PTEN* gene encodes a phosphatase homozygously mutated in a high percentage of human tumors (1, 2). Heterozygous inactivation of *PTEN* results in three human dominant disorders: Cowden disease, Bannayan-Zonana syndrome, and Lhermitte-Duclos syndrome (3). Disruption of *Pten* in the mouse results in early embryonic lethality (4). *Pten* heterozygous (*Pten*^{+/-}) mice display hyperplastic-dysplastic features as well as high tumor incidence (4). The complete penetrance of the hyperplastic-dysplastic changes suggests that these features could be due to *Pten* haploinsufficiency. However, the specific biological consequences of *Pten* haploinsufficiency remain unclear as well as whether complete *Pten* inactivation must occur for full neoplastic transformation. A major substrate of PTEN is phosphatidylinositol trisphosphate (PIP-3), a lipid second messenger produced by PI 3-kinase (5). In the absence of *Pten* activity, PIP-3 concentrations

are increased, leading to enhanced phosphorylation and activation of the survival-promoting factor Akt/PKB (6). *Pten*^{-/-} embryonic stem cells and mouse embryonic fibroblasts are protected from some apoptotic stimuli (6), which suggests that *Pten* can inhibit Akt-dependent survival signals induced in response to PI 3-kinase activation. Here, we show that *Pten* haploinsufficiency results in a lethal autoimmune disorder and that Fas-mediated apoptosis is impaired in *Pten*^{+/-} mice.

Almost 100% of *Pten*^{+/-} females (44 of 45, in the C57BL6/129Sv background) developed, between 4 and 5 months of age, a severe lymphadenopathy affecting mainly the submandibular, axillary, and inguinal lymph nodal stations (Fig. 1A). The mice died, most likely of renal failure (see below), before they were 1 year old. Male mutants were more mildly affected, with 33% of the animals (20 of 24) developing less severe lymph node hyperplasia by 8 months of age and surviving up to at least 15 months.

Gross pathological analysis consistently revealed features that are typically observed in autoimmune disorders:

1) The spleen was enlarged and the lymph nodes were markedly hyperplastic (Fig. 1B). Histological examination (7) showed that

¹Department of Human Genetics-Molecular Biology Program, ²Department of Pathology, Memorial Sloan-Kettering Cancer Center, Sloan-Kettering Institute, 1275 York Avenue, New York, NY 10021, USA. ³Hospital for Special Surgery, Cornell University Medical College, New York, NY 10021, USA.

*To whom correspondence should be addressed. E-mail: p-pandolfi@ski.mskcc.org